Comparing these examples, we can see that the response of both highpass filters are almost equal. Therefore, we can conclude that the Lagrange multiplier method is more efficient in the point of simplicity.

Example 2: The four-band filter bank with high stopband attenuation was designed using the Lagrange multiplier method. The length and the symmetry of each filter are $N_0 = N_1 = N_2 = 40$, $N_3 = 80$, and (SASA). Fig. 4(a) shows a magnitude response of the designed analysis system. The synthesis system is shown in Fig. 4(b).

Example 3: In Example, four-channel LP PR filter banks with the same length was designed by using the Lagrange–Newton method. The specification of these filters is (SASAOOOO), and the length of each analysis filter is 40. Fig. 5(a) and (b) show the frequency response of the analysis and synthesis system, respectively.

VII. Conclusion

In this correspondence, we present two design approaches to design M-channel perfect reconstruction FIR filter banks with linear phase. In the first method, we first design $H_0 \sim H_2$ arbitrarily by using a conventional design method, and then, the highpass filter is designed by using its degrees of freedom. Since this approach does not need any iteration in its design algorithm, the design can be carried out with low computational complexity. However, it has a demerit that the order of a highpass filter becomes high. The second method is a Lagrange–Newton method. In this method, two filters are optimized simultaneously to overcome the problem in the first approach. We also showed a simple way to solve the PR constraint.

References

[1] J. Woods and S. O'Neil, "Subband coding of images," *IEEE Trans. Acoust., Speech, Signal Processing,* vol. ASSP-34, pp. 1278–1288, Oct. 1986.

[2] H. Gharavi and A. Tabatabai, "Sub-band coding of monochrome and color images," *IEEE Trans., Circuits Syst.,* vol. 35, pp. 207–214, 1988.

[3] P. P. Vaidyanathan, *Multirate Systems and Filter Banks.* Englewood Cliffs, NJ: Prentice-Hall, 1993.

[4] T. Q. Nguyen and P. P. Vaidyanathan, "Two-channel perfect-reconstruction FIR QMF structures which yield linear-phase analysis and synthesis filters," *IEEE Trans. Acoust., Speech, Signal Processing,* vol. 37, pp. 676–690, May 1989.

[5] M. Vetterli and D. Le Gall, "Perfect reconstruction FIR filter banks: Some properties and factorizations," *IEEE Trans. Acoust., Speech, Signal Processing,* vol. 37, pp. 1057–1071, July 1989.

[6] P. P. Vaidyanathan, "Theory and design of M-channel maximally decimated quadrature mirror filters with arbitrary M, having the perfect-reconstruction property," *IEEE Trans. Acoust., Speech, Signal Processing,* vol. ASSP-35, pp. 476–492, Apr. 1987.

[7] T. Q. Nguyen and P. P. Vaidyanathan, "Structures for M-channel perfect-reconstruction FIR QMF banks which yield linear-phase analysis filters," *IEEE Trans. Acoust., Speech, Signal Processing,* vol. 38, pp. 433–446, Mar. 1990.

[8] A. K. Soman, P. P. Vaidyanathan, and T. Q. Nguyen, "Linear phase paraunitary filter banks: Theory, factorizations and designs," *IEEE Trans. Signal Processing,* vol. 41, pp. 3480–3496, Dec. 1993.

[9] K. Krosawa, I. Yamada, T. Komou, and N. Yamashita, "Design of a linear phase perfect reconstruction QMF bank," Tech. Rep. IEICE, CAS94-36, VLD94-36, DSP94-58, July 1994.

[10] B.-R. Horng and A. N. Willson, Jr., "Lagrange multiplier approaches to the design of two-channel perfect-reconstruction linear-phase FIR filter banks," *IEEE Trans. Signal Processing,* vol. 40, pp. 364–374, Feb. 1992.

[11] M. Vetterli and C. Herley, "Wavelets and filter banks: Theory and design," *IEEE Trans. Signal Processing,* vol. 40, pp. 2207–2232, Sept. 1992.

[12] M. Vetterli, "Filter banks allowing perfect reconstruction," *Signal Process.,* vol. 10, pp. 219–244, 1986.

[13] P. P. Vaidyanathan and T. Q. Nguyen, "Eigenfilters: A new approach to least-squares FIR filter design and applications including nyquist filters," *IEEE Trans. Circuits Syst.,* vol. 34, pp. 11–23, Jan. 1987.

[14] Y. C. Lim, J.-H. Lee, C. K. Chen, and R.-H. Yang, "A weighted least squares algorithm for quasiequiripple FIR and IIR digital filter design," *IEEE Trans. Signal Processing,* vol. 40, pp. 551–558, Mar. 1992.

[15] T. Nagai and M. Ikehara, "Design of linear phase M channel perfect reconstruction FIR filter banks using Lagrange–Newton method," *Proc. ECCTD95,* vol. 1, 1995, pp. 187–190.

Wavelets for Waveform Coding of Digital Symbols

Prashant P. Gandhi, Sathyanarayan S. Rao, and Ravikanth S. Pappu

***Abstract*—A wavelet-based coder-decoder (codec) structure is defined for baseband waveform coding. Numerical results for bandwidth efficiency are given, and a comparison between several different wavelets is presented. Moreover, it is shown that wavelets obey the Nyquist pulse shaping condition and provide a unified framework for analog pulse shaping concepts of communications.**

I. Introduction

Wavelets have recently become popular in many different scientific fields, including signal processing. A wavelet is a signal or a waveform having desirable characteristics, such as localization in time and frequency, and orthogonality across scale and translation [1], [2]. Because of these appealing properties, wavelets appear to be promising waveforms in communications. Motivation for the use of wavelets for waveform coding stems from the fact that the two ideal waveforms often used to benchmark analog pulse shaping performance, namely, the time-limited rectangular pulse and the band-limited sinc pulse, are the so-called *scaling functions* and have corresponding wavelets. Thus, wavelet theory appears to have the potential for analog pulse shaping applications. We shall see that orthogonality among wavelets and scaling functions makes this a natural connection, and in fact, wavelet theory appears to provide a unified framework for analog pulse shaping.

Specifically, in this correspondence, we use wavelets and the related scaling functions for continuous-time analog representation of data bits. It is shown that the Nyquist pulse shaping criterion is satisfied by wavelets and scaling functions. In fact, it turns out that the bandlimited raised-cosine waveforms are scaling functions of a special class of Meyer wavelets [4]. We should point out that the present application of wavelets employs analog continuous-time wavelets and scaling functions. This is different from the conventional use of wavelet concepts for discrete-time applications, such as data compression, where the wavelet-based approach simply becomes subband coding (see [5]).

Manuscript received December 30, 1994; revised December 16, 1996. The associate editor coordinating the review of this paper and approving it for publication was Prof. Banu Onaral.

P. P. Gandhi is with Advanced Audio Design, Texas Instruments, Inc., Dallas, TX 75243 USA (e-mail: gandhi@ti.com).

S. S. Rao is with the Department of Electrical and Computer Engineering, Villanova University, Villanova, PA 19085 USA.

R. S. Pappu is with the Spatial Imaging Group, Media Laboratory, Massachusetts Institute of Technology, Cambridge, MA 02139 USA.

Publisher Item Identifier S 1053-587X(97)06436-2.

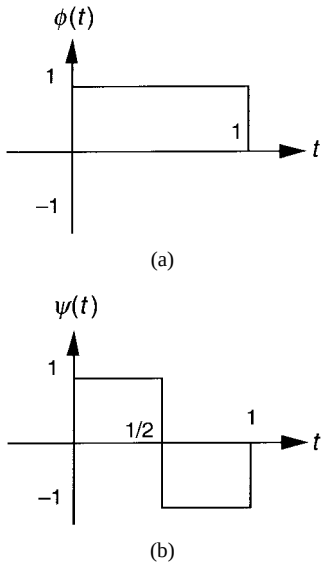

Fig. 1. (a) Haar (D2) scaling function. (b) Haar wavelet.

II. Preliminaries

Briefly, let $\psi(t)$ be a (mother) wavelet. A dilated (or scaled) and translated wavelet $\psi_{j,k}(t)$ is given by $\psi_{j,k}(t) = 2^{-j/2}\psi(2^{-j}(t - 2^j k))$, where 2^j and $2^j k$ indicate the amount of dilation and translation for some integers j and k. It can be shown that the inner product between $\psi_{j,k}(t)$ and $\psi_{m,n}(t)$ for some integers j, k, m, n is given by

$$\langle \psi_{j,k}(t), \psi_{m,n}(t) \rangle = \int_{-\infty}^{\infty} \psi_{j,k}(t)\psi_{m,n}(t)\,dt = \delta_{j-m}\delta_{k-n} \quad (1)$$

which implies that dilated and translated wavelets $\psi_{j,k}(t)$ for different (j,k) values are orthogonal to each other. Wavelets are unit-energy bandpass functions. There also exist corresponding unit-energy lowpass functions, called *scaling functions* $\phi_{j,k}(t)$, which are generated from a mother function $\phi(t)$. Orthogonality relations

$$\begin{aligned} \langle \phi_{j,k}(t), \phi_{j,n}(t) \rangle &= \delta_{k-n} \\ \langle \psi_{j,k}(t), \phi_{m,n}(t) \rangle &= 0, \quad j \le n \end{aligned} \quad (2)$$

imply that scaling functions, for a given dilation, are orthogonal across translation, whereas wavelets and scaling functions are orthogonal at certain dilations and arbitrary translations. Additionals details and properties of wavelets may be found in [2].

There exist many families of wavelets and scaling functions. For example, the well-known Haar wavelet (see Fig. 1) is given by $\psi(t) = 1/2$ for $0 \le t < 1/2$ and $= -1/2$ for $1/2 \le t < 1$ and has corresponding scaling function $\phi(t) = 1$ for $0 \le t < 1$. Note that both the Haar wavelet and the corresponding scaling function are commonly used to represent digital information in communication systems where the Haar scaling function is generally referred to as the full-width rectangular pulse and the Haar wavelet as the biphase pulse.

Due to the discontinuity, however, the spectrum of the Haar wavelet does not decay rapidly. Wavelets that are smoother than the Haar wavelet do exist, and they offer better temporal-spectral tradeoffs. We consider two well-known wavelet families in this correspondence; they are commonly referred to as Daubechies family of wavelets and Lemarie–Battle wavelets.

The Haar wavelet is an extreme example of Daubechies family of wavelets [2]. A Daubechies mother wavelet D_M of order M, $M \ge 2$ and even, has *finite* temporal support in $[0, M-1]$, and its spectrum decays polynomially. The wavelet D_2 is the Haar function and is the only discontinuous wavelet of this family. As the order M increases, the D_M wavelet becomes increasingly smoother and longer. The Lemarie–Battle wavelet, on the other hand, is defined using cubic spline functions and is neither time limited nor bandlimited (see [1]). However, it decays polynomially in time and exponentially in frequency.

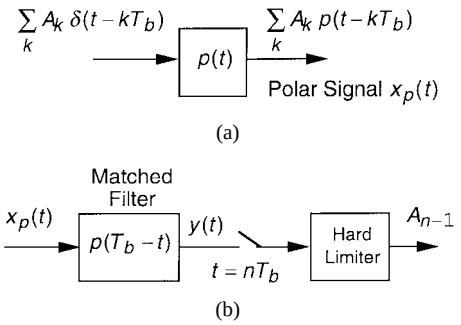

Fig. 2. Block diagram of baseband polar codec. (a) Transmitter. (b) Receiver.

III. Waveform Coding Using Scaling Functions and Wavelets

In this section, we first discuss the traditional (rectangular-pulse) polar signaling technique used for binary phase shift keying (BPSK). A BPSK codec based on scaling functions is then described, followed by a two-channel BPSK codec based on *both* scaling functions and wavelets. Finally, bandwidth efficiency is computed for signaling schemes under consideration, and comparisons are made. We note that the use of strictly bandpass wavelets for baseband coding has been proposed in [6] under the fractal modulation framework, where results are presented using the ideal bandlimited "sinc" waveform. In addition, bit-by-bit coding using discrete shift-orthogonal wavelet sequences has been recently considered in [7], whereas application of wavelets for secure communications has been studied in [8] and [9].

In the traditional BPSK modulator (see Fig. 2), polar signaling is used to encode each bit prior to modulation. That is, a binary "1" is represented by a pulse $p(t)$ of duration T_b, and a binary "0" is represented by $-p(t)$. This polar signaling scheme is efficient in that for given bit energy, it provides maximum separation between the two bit signals and thus yields the lowest probability of bit error among other binary modulation schemes (on-off, orthogonal, etc.).

Let $\{A_k\}$ be a sequence of statistically independent symbols, each assuming the value $\sqrt{E_b}$ for bit "1" or $-\sqrt{E_b}$ for bit "0," where E_b is the bit energy. A polar (baseband) signal based on pulse $p(t)$ may then be represented as

$$x_p(t) = \sum_{k=-\infty}^{\infty} A_k p(t - kT_b) \quad (3)$$

where T_b is the bit duration ($R_b = 1/T_b$ is the bit rate), and $p(t)$ is a unit-energy continuous-time pulse of duration T_b (e.g., the full-width rectangular pulse). In the presence of additive white Gaussian noise, the optimum receiver is a matched filter with impulse response function $p(T_b - t)$ followed by a sampler and a hard limiter. For BPSK, baseband signal (3) is used to modulate the carrier $\cos(\omega_c t)$, where ω_c is the carrier frequency.

With $p(t)$ being the full-width rectangular pulse, we may say that information bits in (3) are coded using the D_2 (or Haar) scaling function. This D_2 scaling function, however, does not have appealing spectral characteristics; therefore, it is natural to consider other scaling functions that do have desirable characteristics. Replacing $p(t)$ in (3) with a suitable scaling function $\phi(t)$, we get

$$x_\phi(t) = \sum_{k=-\infty}^{\infty} \frac{A_k}{\sqrt{T_b}} \phi\left(\frac{t - kT_b}{T_b}\right). \quad (4)$$

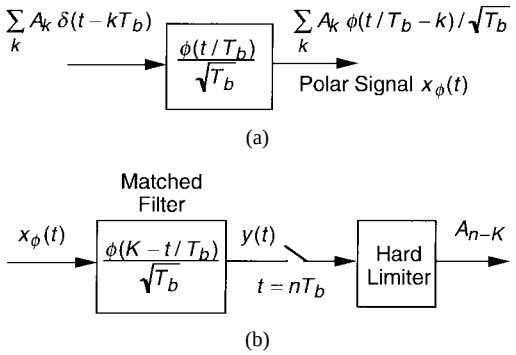

Fig. 3. Block diagram of codec based on scaling function. (a) Transmitter. (b) Receiver.

Note that each scaling function in (4) is dilated by T_b. Since typical $\phi(t)$ has temporal support larger than unity (except for D_2), the dilated scaling function in (4) has temporal duration $T > T_b$. A D_M scaling function, for example, is of duration $T = (M-1)T_b$. Block diagrams of a scaling function-based baseband modulator and demodulator are given in Fig. 3. Fig. 4(a) shows a typical polar signal representing bit sequence $\cdots$ 1 0 0 1 $\cdots$. The same bit sequence, which has been coded using D_4 scaling functions, is shown in Fig. 4(b).

Since information bits arrive at rate $R_b = 1/T_b$, it is easy to see that scaling functions corresponding to neighboring bits *overlap*. This is evident from Fig. 4(b). The resulting polar signal is depicted in Fig. 4(c). Decoding of bits is possible because, according to (2), any pair of scaling functions separated by integer multiple of T_b are orthogonal. Specifically, at the receiver (see Fig. 3), impulse response of the matched filter is given by $\phi(\frac{KT_b-t}{T_b})/\sqrt{T_b}$, where $T = KT_b$ is the duration of $\phi(t/T_b)$ for some integer $K \geq 1$. Assuming a noiseless transmission medium, the matched filter output $y(t)$ sampled at $t = nT_b$ is

$$\begin{aligned} y(t=nT_b) &= x_\phi(t) * T_b^{-1/2}\phi\left(\frac{KT_b-t}{T_b}\right)\Big|_{t=nT_b} \\ &= \sum_{k=-\infty}^{\infty}\frac{A_k}{T_b}\int_{(n-K)T_b}^{nT_b}\phi\left(\frac{\tau-kT_b}{T_b}\right)\phi\left(\frac{\tau-(n-K)T_b}{T_b}\right)d\tau \\ &= A_{n-K}. \end{aligned} \tag{5}$$

Clearly, from (5), information bits are recovered at the receiver at rate R_b after an initial delay of KT_b, as seen from Fig. 4(d).

Bit error probability (BER), in the presence of additive white Gaussian noise, can also be computed easily. For shift-orthogonal waveforms $\phi(t/T_b)$, the receiver BER can be calculated from the BPSK (or polar) signal space diagram. It is therefore not surprising to see that for equal bit energies, the BER for (4) is *identical* to the one for (3). Hence, comparison between the two methods should only be based on their bandwidth utilizations.

Before proceeding to the determination of bandwidth efficiencies, we list some key features of the scaling function-based waveform coding technique:

- Neighboring waveforms overlap.
- Decoder outputs are delayed by KT_b.
- Output bit rate is identical to the input rate.
- BER is equal to the BER of BPSK scheme.

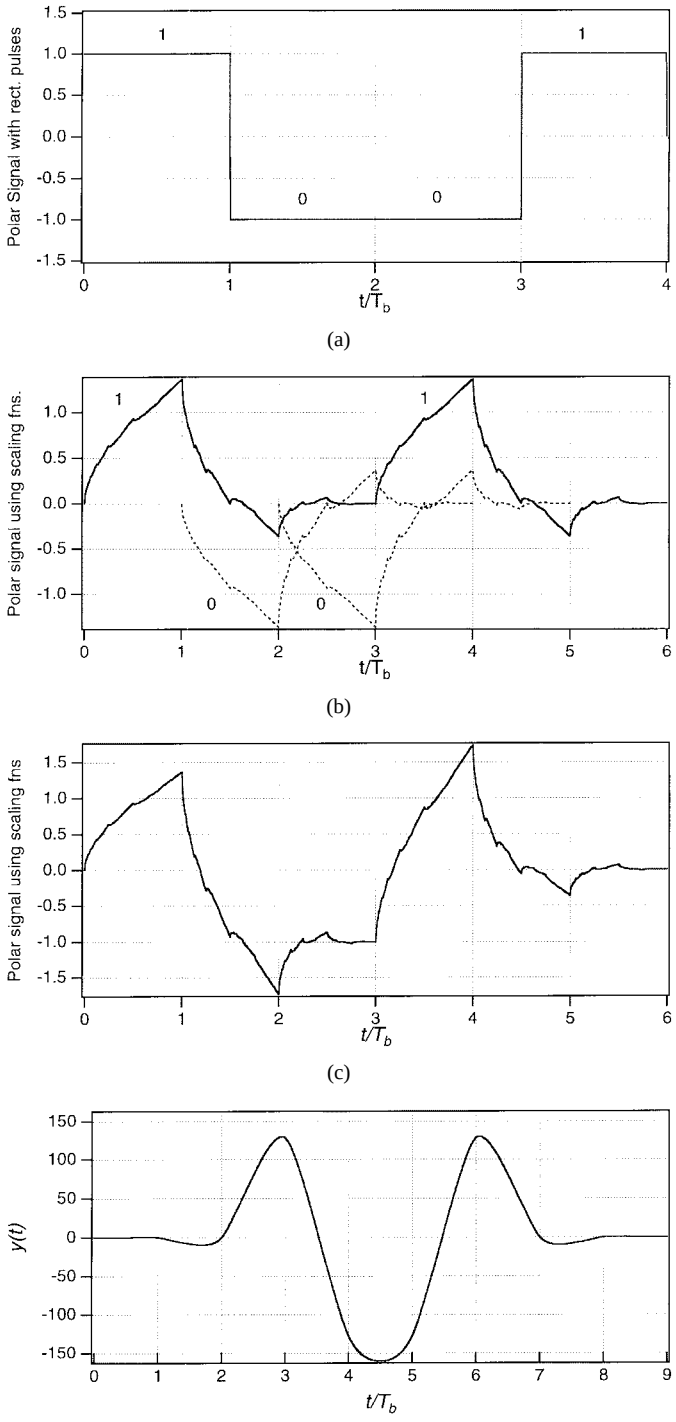

Fig. 4. (a) Polar signal using rectangular pulses. (b) D4 scaling functions corresponding to information bits 1 0 0 1. (c) Polar signal using D4 scaling function. (d) Matched filter output.

The above scheme can be generalized to include both scaling functions and wavelets as shown in Fig. 5. Here, the composite baseband signal is a sum of two polar signals—one coded using scaling functions and the other using wavelets:

$$x_{\phi\psi}(t) = \sum_{k=-\infty}^{\infty}\frac{A_k}{\sqrt{T_b}}\phi\left(\frac{t-kT_b}{T_b}\right) + \sum_{k=-\infty}^{\infty}\frac{B_k}{\sqrt{T_b}}\psi\left(\frac{t-kT_b}{T_b}\right). \tag{6}$$

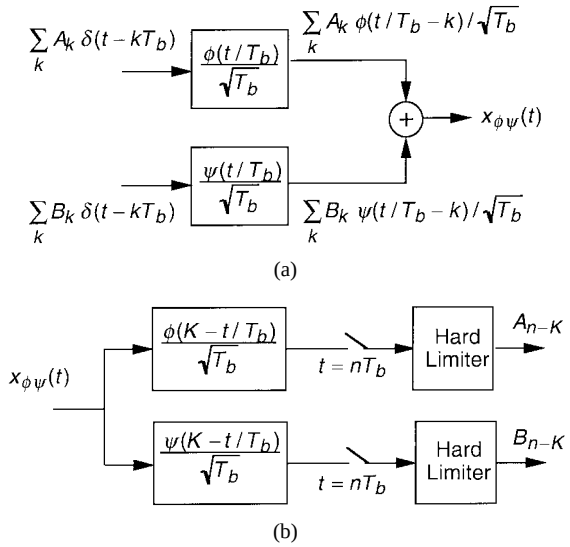

Fig. 5. Block diagram of codec based on scaling function and wavelet. (a) Transmitter. (b) Receiver.

TABLE I
BANDWIDTH EFFICIENCY FOR SEVERAL DIFFERENT WAVEFORMS

Wavelet	BW (Hz)	BE (bits/s/Hz)
D_2 (Haar)	3.5	0.57
D_4	3.1	0.65
D_6	2.8	0.71
D_8	1.4	1.43
D_{10}	1.35	1.48
Lemarie–Battle	1.15	1.74

The zero-mean random variables $\{A_k\}$ and $\{B_k\}$ in (6) are assumed to be individually and jointly independent. A corresponding passband signal is obtained by modulating a single carrier $\cos(\omega_c t)$ using (6). Note that the signal constellation in this case is identical to the four-symbol biorthogonal or quadrature phase shift keying (QPSK) technique. Decoding is possible, as shown in Fig. 5, due to the self- and cross-orthogonality properties of the $\phi(t/\sqrt{T_b})$ and $\psi(t/\sqrt{T_b})$ functions. The bit error rate again remains equal to the BPSK scheme as we are dealing with two independent polar signals [3]. Further, the data rate is doubled as is the overall bandwidth.

To compare different wavelet-based coding techniques, we employ the bandwidth efficiency (BE) measure defined by

$$\text{BE} = \frac{\text{Total Bit Rate}}{\text{Bandwidth}} \text{ (bits/s/Hz)} \tag{7}$$

where we assume 99% power bandwidth.[1] Numerical comparisions are given in the Table I. Here, the 99% bandwidth (BW) is normalized with respect to the bit period T_b. As seen from Table I, BE improves with higher orders of Daubechies waveforms; Lemarie–Battle waveforms give the best performance.

IV. WAVELETS AND ZERO ISI WAVEFORMS

By expressing the shift orthogonal property of scaling functions $\phi(t/T_b)$ in the frequency domain, we get

$$\sum_{k=-\infty}^{\infty}\left|\Phi\left(\omega-\frac{2\pi k}{T_b}\right)\right|^2 = T_b \tag{8}$$

where $\Phi(\omega)$ is the continuous-time Fourier transform of $\phi(t)$. We see that (8) is the Nyquist pulse shaping condition for zero intersymbol interference (ISI) with the receive waveform matched to the bandlimited transmit waveform $\phi(t/T_b)$ (see [3]). This connection between wavelet theory and analog pulse shaping concepts of communications is remarkable [4], [10]. It suggests that bandlimited raised-cosine pulses are related to scaling functions of some suitable family of wavelets. In fact, in [4], it is shown that the square-root raised cosine pulse is a special case of the bandlimited Meyer family of wavelets. We also note that *biorthogonal*[2] wavelets (as opposed to *orthogonal* wavelets considered in this correspondence) have recently been applied to partial response channels [11].

Thus, continuous-time wavelet theory appears to provide a unified framework for analog pulse shaping. All orthogonal scaling functions and wavelets known to date are candiates for pulse shaping, each giving certain temporal and spectral tradeoffs. Of course, the chosen waveform must meet the design requirements such as spectral and temporal decay, amount of ISI and timing errors allowed, and amount of phase and frequency deviation tolerated. Although the specific choice of wavelet is application-dependent, no analytical or *ad hoc* design rules exist to pick a good wavelet for a given application.

Even if one were to develop a set of guidelines that identify the wavelet most suitable for given specifications, physical means to generate this analog continuous-time wavelet are not yet available. It is well known that a continuous-time wavelet or scaling function can be generated by infinitely cascading a prototype FIR or IIR discrete-time filter [1], [2]. However, in reality, even a finite cascade may be neither practical nor cost effective. We should not be discouraged by this; in fact, the conventional scaling functions, i.e., full-width rectangular function and the sinc function, cannot be generated precisely. Methods to produce acceptable approximations of these waveforms have been engineered in the past. Similarly, we must look for ways to approximate those scaling functions and wavelets that promise improved performance-versus-cost metric.

REFERENCES

[1] S. Mallat, "A theory of multiresolution signal decomposition: The wavelet representation," *IEEE Trans. Pattern Anal. Machine Intell.*, vol. vol. 11, pp. 674–693, July 1989.
[2] I. Daubechies, *Ten Lectures on Wavelets*. Philadelphia, PA: SIAM, 1992.
[3] J. Proakis and M Salehi, *Communication Systems Engineering*. Englewood Cliffs, NJ: Prentice-Hall, 1994.
[4] W. Jones, "A unified approach to orthogonally multiplexed communication using wavelet bases and digital filter banks," Ph.D. dissertation, Ohio Univ., Athens, Aug. 1994.
[5] A. Akansu, "Wavelets and filter banks: A signal processing perspective," *IEEE Circuits Devices Mag.*, pp. 14–18, Nov. 1994.
[6] G. Wornell and A. Oppenheim, "Wavelet-based representations of a class of self-similar signals with application to fractal modulation," *IEEE Trans. Inform. Theory*, vol. 38, pp. 785–800, Mar. 1992.
[7] M. Tzannes and M. Tzannes, "Bit-by-bit channel coding using wavelets," in *Proc. GLOBECOM*, 1992.
[8] D. Cochran and C. Wei, "Scale based coding of digital communication signals," in *Proc. IEEE-SP Int. Symp. Time-Freq. Time-Scale*, Oct. 1992, pp. 455–458.
[9] R. Orr *et al.*, "Covert communications employing wavelet technology," in *Proc. 27th Asilomar Conf. Signals, Syst., Comput.*, Nov. 1993.
[10] P. Gandhi, "Wavelet sampling of continuous-time signals," in *Proc. Conf. Inform. Sci. Syst.*, Baltimore, MD, Mar. 1995.
[11] M. Raghuveer, "Wavelets as signaling waveforms over partial response channels," in *Proc. SPIE Photonics Conf. Coding Signal Process. Inform. Storage*, Philadelphia, PA, Oct. 1995.

[1] The 99% power bandwidth W (in Hz) of $x_p(t)$ is numerically obtained from $0.99\int_{-\infty}^{\infty}|P(\omega)|^2\,d\omega = \int_{-2\pi W}^{2\pi W}|P(\omega)|^2\,d\omega$ [3].

[2] In wavelet theory, the term *biorthogonal* has meaning different from that used in communications.